ARTICLES

Two-Dimensional Assemblies of Banana-Shaped Liquid Crystal Molecules on HOPG Surface

Jian-Ru Gong† and Li-Jun Wan*

Institute of Chemistry, Chinese Academy of Sciences (CAS), Beijing 100080, China

Received: May 17, 2005; In Final Form: August 5, 2005

Two-dimensional assemblies of a series of banana-shaped liquid crystal molecules, 1,3-phenylene bis[4-(4-*n*-alkylphenyliminomethyl) benzoates] (P-*n*-PIMB, $n = 12, 14, 18$), are investigated on a highly oriented pyrolytic graphite (HOPG) surface by using scanning tunneling microscopy (STM) at a submolecular level in an ambient environment. Two types of molecular arrangements are observed in these self-assemblies with different stripe widths that resulted from the organization of the alkyl chains. The polarization of the P-*n*-PIMB monolayers is exactly compensated by the adjacent lamellae with opposite bent direction. Furthermore, a bilayer structure is found in the assembly of P-18-PIMB molecules. In comparison with a gemini surfactant molecule, 4,4′-di[4-(octadecylmethylamino)styryl]-1,1′-pentamethylenebispyridinium dibromide (OPD), P-*n*-PIMB molecules appear in more complicated packing arrangements. The results in this paper demonstrate the effects of the molecular structures on the adlayer arrangement and will be helpful in fabricating two-dimensional molecular structures on solid surfaces.

Introduction

Liquid crystals (LCs) are drawing attention from the areas of organic light-emitting devices, photovoltaics, and thin film transistors, and so forth, due to their high carrier mobilities, the anisotropic transport, and polarized emission resulting from the self-assembling properties and supermolecular structures (phases) of LCs.[1,2] Classical thermotropic liquids are commonly composed of rodlike molecules and disk-shaped molecules. However, the banana-shaped LCs represent a new sub-field of LCs. Because of the sterically induced packing of the bent molecules, new smectic modifications can occur which have no counterpart in the field of calamitic LCs. On the other hand, the unconventional molecular structure can lead to unusual physical properties. The polar packing of the bent molecules with C_{2v} symmetry gives rise to ferro- or antiferroelectric properties.[3] Ferroelectricity results from the characteristic layer packing of banana-shaped molecules in which their bent direction is uniformly aligned within layers. Its packing symmetry is a polar C_{2v}, and the polarization appears along the bent direction of molecules.[4] Ferroelectrics have a variety of practical application, such as piezo- and pyroelectricity, second-order nonlinear optical activity, and fast-switching electrooptical devices.[5]

Although the characteristics of bulk banana-shaped LCs have been studied in great detail by techniques such as differential scanning calorimetry (DSC), X-ray diffraction (XRD), the polarizing optical microscope, and nuclear magnetic resonance (NMR),[6] the microscopic structural analysis in the two-dimensional (2D) film form of these molecules has scarcely been made. For the 2D system, the free-standing smectic LC film, which is free from the influence of a substrate, is regarded as a most promising system to study the 2D crystalline order.[7] Some ferroelectric thin film research results were interpreted as bulk ferroelectricity suppressed by surface depolarization energies and imply that the bulk transition has a minimum critical size. Bune et al. observed a first-order ferroelectric phase transition with a transition temperature nearly equal to the bulk value, even in those almost 2D films.[8,9] This result challenges theoretical predictions that the transition temperature should decrease and ferroelectricity vanish in films below a minimum critical thickness; Also it indicates that the surface layers have a preferred direction controlled by the interaction with the substrate or the top electrode,[10] and the orientation of polar molecules in LC thinner films can be modulated on a relatively short time scale using a small electric field.[11]

To further understand the novel properties in these LC systems, the study of the microscopic organization and critical phenomena of these molecules is important. One of the powerful sample preparation techniques for this purpose is the self-assembly technique, which is a critical and necessary process in natural biological systems and of ever-increasing importance in chemistry and material science.[12]

Scanning tunneling microscopy (STM) gives rise to the local character of STM measurements, which makes it possible to visualize surface structure with sub-angstrom resolution and detect various atomic-scale details that are inaccessible by diffraction and spectroscopic techniques.[13−17] The STM study of LC molecules on graphite and MoS_2 had been reported by several research groups.[18−26] The effect of alkyl chain length on the packing structure of the discotic LC triphenylene monolayer has been investigated.[18−25] The STM map of the

* Corresponding author. Tel. & Fax: +86-10-62558934. E-mail: wanlijun@iccas.ac.cn.
† Also in CAS Graduate School.

10.1021/jp052581q CCC: $30.25
Published on Web 09/15/2005

interfacial structure of the antiferroelectric LC phase revealed that the antiferroelectric layers consist of novel quadruple "zigzag" molecular rows.[26]

In the present paper, we present an STM study on the spontaneously formed adlayers of banana-shaped LC molecules on a HOPG surface and their assembling behavior. As a comparison, the assembling structure of a gemini surfactant OPD is also provided. The effects of the chemical structure of molecules on the adlayer structure are discussed.

Experimental Section

Achiral banana-shaped molecules, 1,3-phenylene bis[4-(4-*n*- alkylphenyliminomethyl)benzoates] (P-*n*-PIMB, $n = 18$, 14, and 12),[3] and the gemini surfactant molecule 4,4′-di[4-(octadecylmethylamino)styryl]-1,1′-pentamethylenebispyridinium dibromide (OPD) were synthesized according to the literature.[27,28] The chemical structures of the compounds are shown in Chart 1. The adlayer was prepared by placing a drop (2 μL) of chloroform (HPLC grade, Aldrich) solution containing the compound in a concentration of approximately 10^{-6} M on a freshly cleaved atomically flat surface of highly oriented pyrolytic graphite (HOPG, quality ZYB).

CHART 1: Chemical Structures of the Compounds

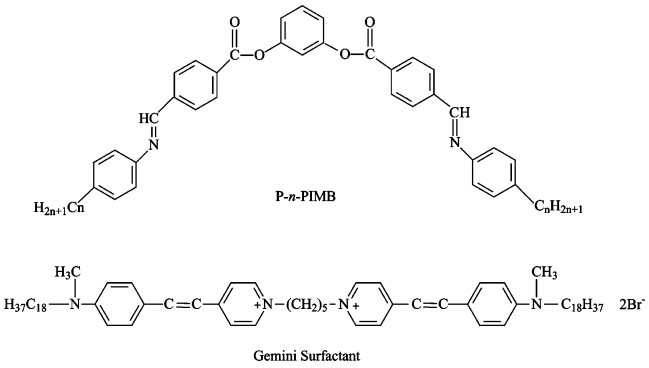

A Nanoscope IIIa SPM (Digital Instruments, Santa Barbara, CA) was employed to carry out the STM experiments using a standard constant-current mode under atmosphere. The tunneling tips used were mechanically cut Pt/Ir wire (90/10). All the STM images are presented without further processing. The tunneling conditions used are given in the corresponding figure captions.

Results and Discussion

1. P-18-PIMB Adlayer. *Chiral Domains.* P-18-PIMB molecules spontaneously adsorb on the HOPG surface and self-organize into a two-dimensional (2D) assembly with a well-defined structure. An STM image reveals the ordered topography of P-18-PIMB molecules with remarkably bright bands and dark stripes alternating over the whole viewed area. Two types of domains could be observed, named arrangement types I and II. For type I, a typical STM image is shown in Figure 1a. The adsorption arrangement with the same dark stripe width can be observed in the image. Owing to the large electronic density of aromatic rings, the aromatic part of the molecule appears in higher contrast than the alkyl chains in the image. Thus, it is reasonable to attribute the bright bands to the aromatic parts of the molecules. The detail of the adlayer is seen in Figure 1b. Each of the five aromatic rings appears as a bright spot, forming a banana-shaped configuration. Beside the bright spots, the darker regions correspond to the alkyl side chains of the molecules. The length of one alkyl side chain is measured to be 2.3 ± 0.2 nm, corresponding to the length of an octadecyl

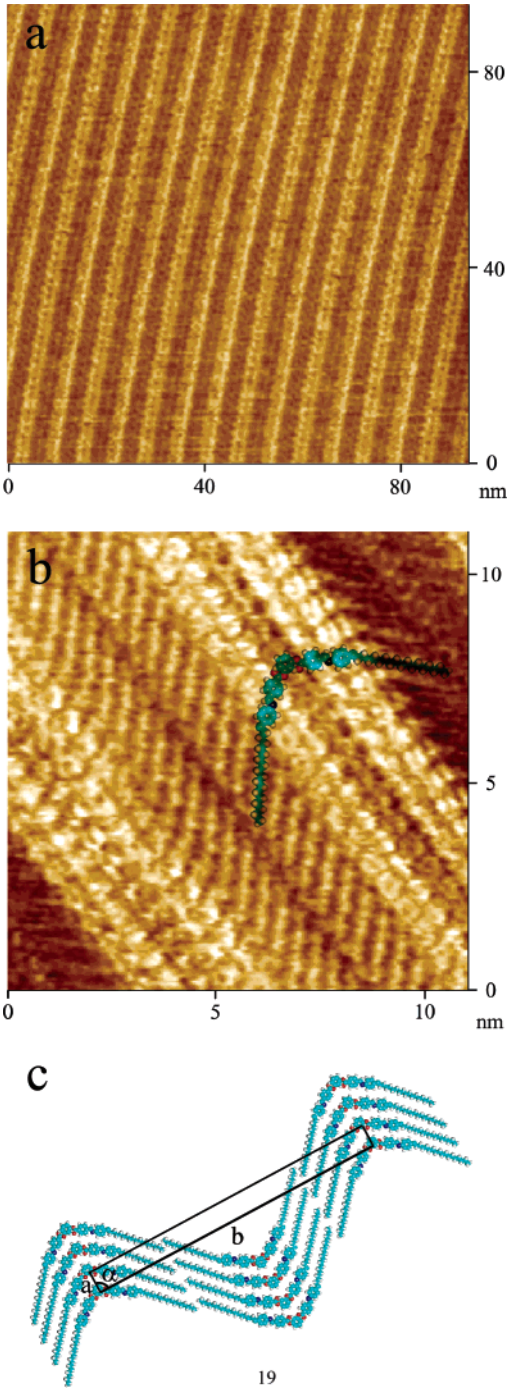

Figure 1. Type I adsorption geometry of P-18-PIMB molecules on the HOPG surface showing a flat-lying orientation. (a) Large-scale STM image recorded with $V = 898$ mV, $I = 316$ pA. (b) High-resolution STM image recorded with $V = 931$ mV, $I = 864$ pA. (c) Structural model for the type I arrangement.

chain. From the structural information in the STM image, a molecular model is superimposed in Figure 1b. The high-resolution image reveals that the alkyl side chains in the adjacent lamellae all adopt a tail-to-tail packing geometry. Owing to the molecular orientation on the HOPG surface, two side alkyl chains in a lamella show different contrast in the STM image. Observed from the image, the adjacent molecules in a lamella are parallel to each other with a uniform bent direction, while the molecules in the neighboring lamellae adopt an antiparallel packing pattern. The molecular arrangement model and a unit cell are depicted in Figure 1c. The parameters in a unit cell are

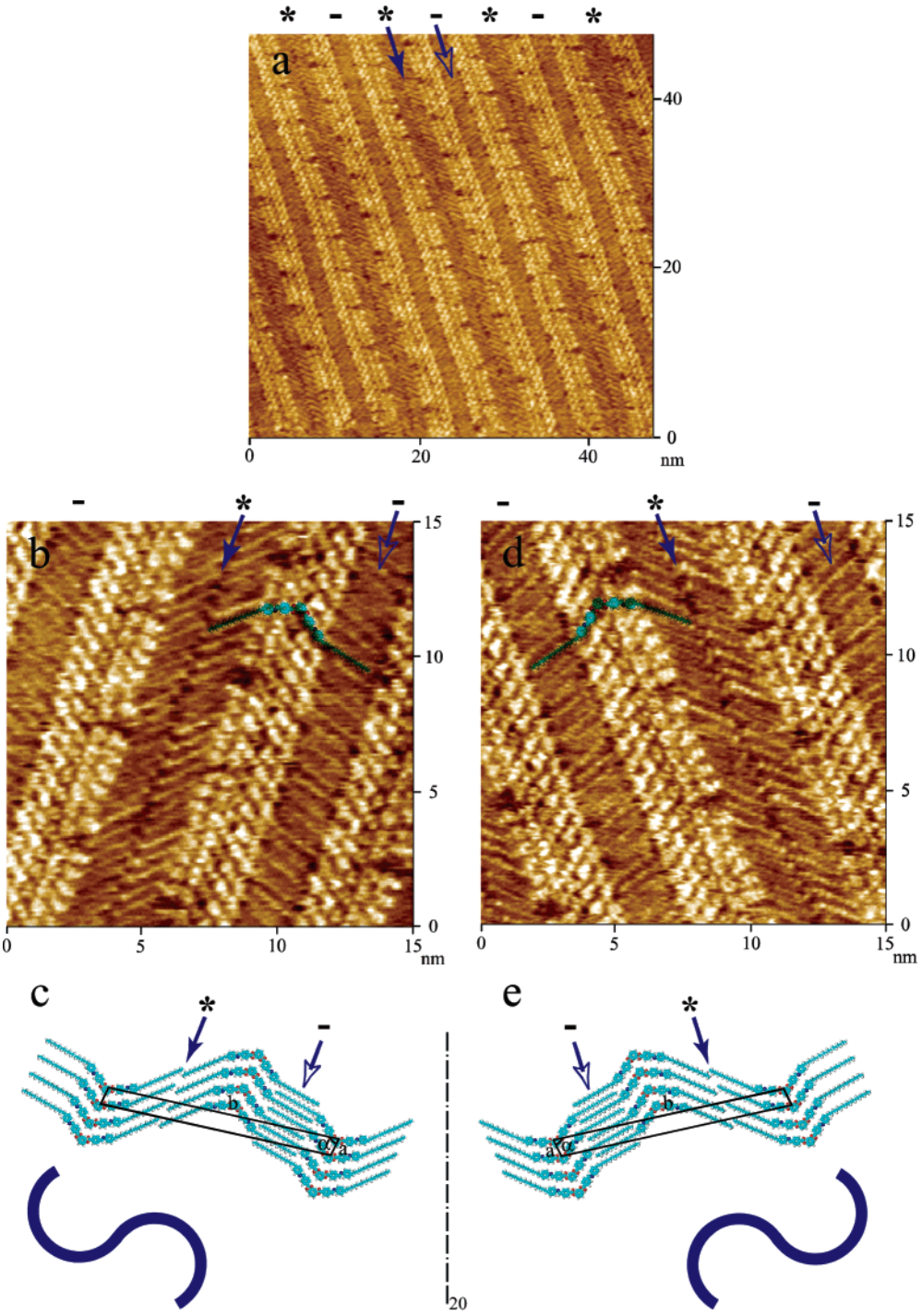

Figure 2. Type II adsorption geometry of P-18-PIMB molecules on HOPG showing a flat-lying orientation. (a) Large-scale STM image recorded with $V = 898$ mV, $I = 316$ pA. (b) and (d) High-resolution STM images showing mirror chiral structures by achiral molecules recorded with (b) $V = 812$ mV, $I = 658$ pA, and (d) $V = 898$ mV, $I = 187$ pA. (c) and (e) Structural models for the type II arrangements in (b) and (d), respectively.

$a = 0.8 \pm 0.2$ nm, $b = 11.5 \pm 0.2$ nm, and $\alpha = 85 \pm 2°$, consistent with the results from STM measurement.

Another molecular arrangement of P-18-PIMB, type II, is shown in Figure 2a. In this image, the narrow dark stripes marked by (-) and the wide dark stripes with a trough in the middle marked by (∗) exist alternately. The alkyl side chains on different stripes of the molecules adopt different packing patterns. The details are seen in Figure 2b. On the (∗) side, they are packed tail-to-tail with the alkyl side chains of the neighboring lamella separated by a narrow dark trough; on the (-) side, the alkyl side chains of adjacent lamellae fully interdigitate with each other. The molecular arrangement could be seen more clearly from the molecular packing model shown in Figure 2c. The parameters of a unit cell are $a = 0.8 \pm 0.2$ nm, $b = 11.0 \pm 0.2$ nm, and $\alpha = 80 \pm 2°$, respectively. In addition, changing the observation area, the chiral domains formed by the achiral molecules could be observed. Figure 2d is the mirror high-resolution STM image having the same unit cell parameters with its symmetrical packing of Figure 2b. Taking the tail-to-tail alkyl packing stripe (∗) as the central axis, the molecular bent directions constitute an "S" shape in Figure 2c, while an inverted "S" shape for the mirror packing in Figure

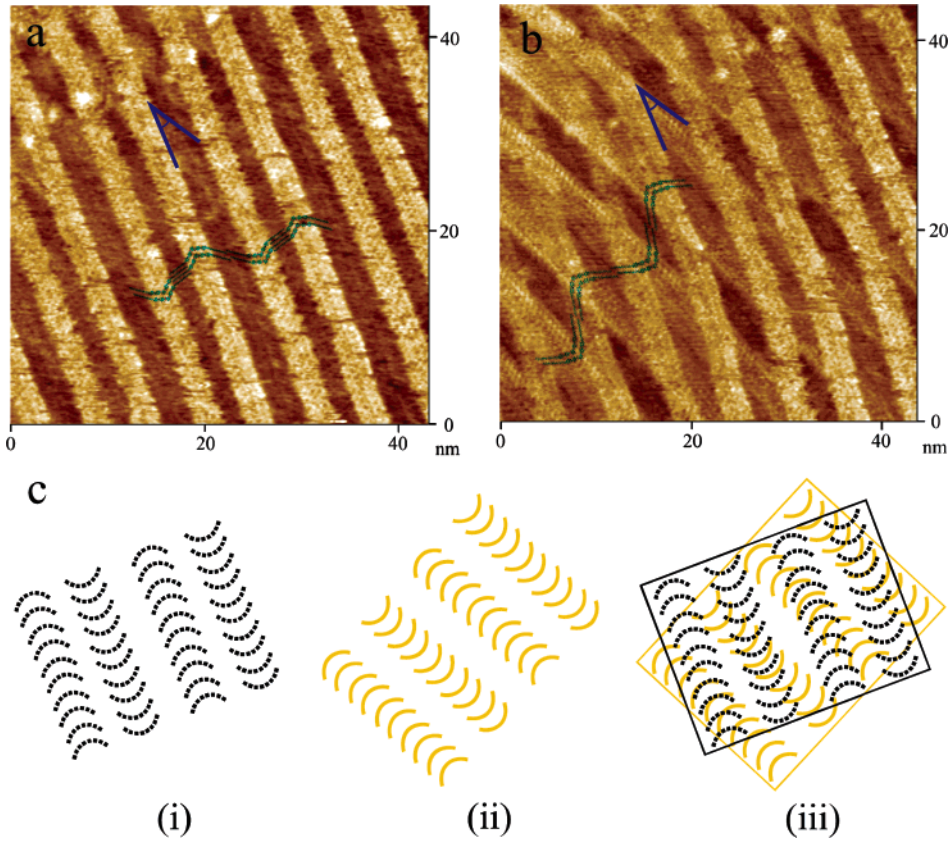

Figure 3. STM image of the P-18-PIMB bilayers recorded with (a) $V = 812$ mV, $I = 658$ pA, (b) $V = 739$ mV, $I = 658$ pA. (c) Schematic illustrations of (i) the top monolayer; (ii) the adjacent lower monolayer, and (iii) the bilayers.

2e. This result gives direct evidence for the existence of 2D chiral domains formed by the banana-shaped achiral molecules.

Bilayer. A bilayer structure of P-18-PIMB adlayers was observed by STM in this research. Although the image is not well-reproducible, it is a real structure. A typical image is shown in Figure 3a. The different lamellae in the top and lower layers cross each other at an angle of about 30°, as marked on the image. Judged from the dark stripe widths and alkyl chain packing structures, the top monolayer adopts the type II arrangement, and the molecular alignment of the monolayer is simply illustrated in Figure 3c(i). Decreasing STM imaging bias, the adjacent lower monolayer in the bilayer could be more clearly seen in Figure 3b, and the type I arrangement could be determined through the lamellae interspacing measurement and the alkyl side chain packing pattern. Figure 3c(ii) schematically describes the molecular alignment of the lower monolayer. A structural model of the bilayers is shown in Figure 3c(iii) and shows the relative orientation between the top and lower adlayers.

The research results reported by Tang et al. indicate that the monolayer islands of three-ring bent-core compounds are unstable and easy to transform to slender bilayer crystals at room temperature.[29] For the banana-shaped molecules of P-*n*-PIMB, the helical domains are formed in the SmA_b phase.[30] Khachaturyan has shown theoretically that a liquid ferroelectricity cannot exist in a homogeneous nematic state and be transformed into a more stable helical structure. In our case, the formation of the bilayer might be considered as a soft-mode instability of LC thin film. It should be pointed out that the bilayer structure in the present study is only observed in the assembly of P-18-PIMB. Further experiments and theoretical studies are necessary to conclude the reasonable origin of the bilayer formation.

2. P-14-PIMB Adlayer. To investigate the effect of chemical structure of molecules on the assembling structure, we prepared a P-14-PIMB adlayer on HOPG and observed the change in the adlayer structure. Similar to P-18-PIMB, two types of molecular arrangements are also observed in the P-14-PIMB adlayer. The arrangement of type I for the P-14-PIMB adlayer is shown in a large-scale defect-free STM image in Figure 4a. The tail-to-tail alkyl side chains could be clearly seen in the high-resolution STM image of Figure 4b. Figure 4c is a proposed molecular packing model from STM results. The unit cell parameters in the adlayer are $a = 0.8 \pm 0.2$ nm, $b = 10.6 \pm 0.2$ nm, and $\alpha = 87 \pm 2°$, shown in Figure 4c.

For arrangement type II, P-14-PIMB molecules form a well-ordered organization with bright bands and dark stripes alternately in a large area, as shown in Figure 5a. The alternately homogeneous narrow dark stripes (-) and the wide dark stripes (∗) with a trough appear in the adlayer. The structure is similar to that in the arrangement type II of P-18-PIMB. The high-resolution STM image in Figure 5b shows the details of the molecular arrangements in the different stripes. A molecular model is superimposed in Figure 5b. It can be seen from the image, on the (-) side of the lamellae, the alkyl side chains fully interdigitate each other. On the other side (∗) of the lamella, the alkyl side chains of adjacent lamellae are packed with a tail-to-tail arrangement. The molecular packing model is tentatively proposed in Figure 5c, consistent with the results of STM measurement. The parameters in the unit cell are recognized as $a = 0.8 \pm 0.2$ nm, $b = 10.3 \pm 0.2$ nm, and $\alpha = 81 \pm 2°$. For the two types of arrangements, the molecular bent direction of lamellae is invariable in every second neighboring lamellae but opposite to the other between the neighboring lamellae. For P-14-PIMB molecules, the chiral domains formed

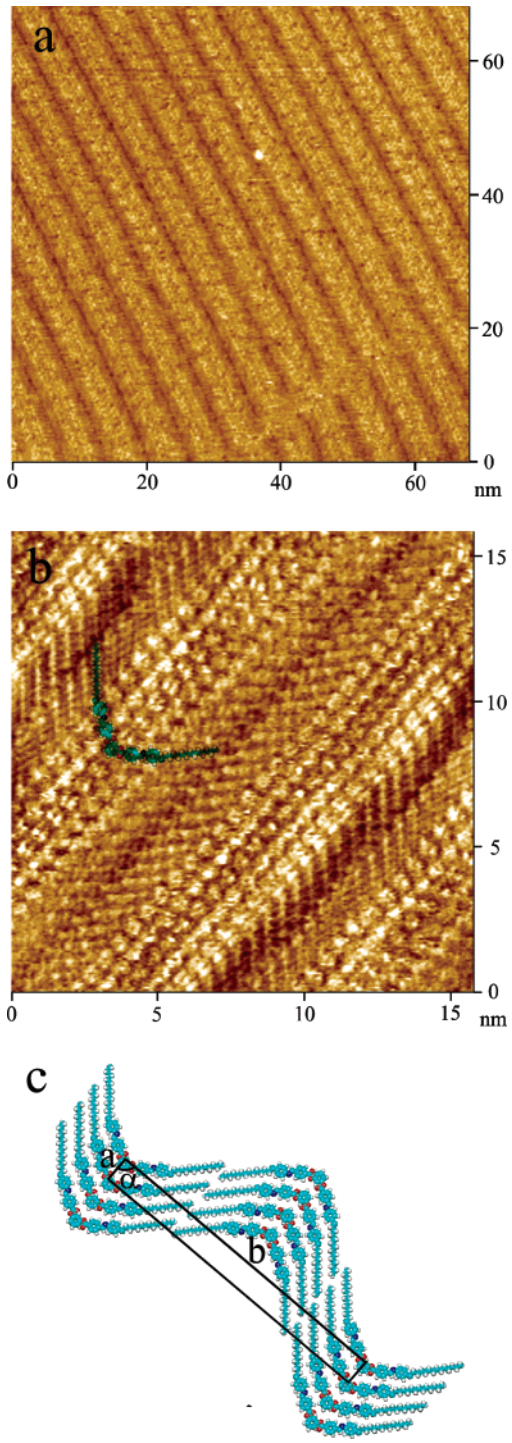

Figure 4. Type I adsorption geometry of P-14-PIMB molecules on the HOPG surface. (a) Large-scale STM image recorded with $V = 964$ mV, $I = 432$ pA. (b) High-resolution STM image recorded with $V = 600$ mV, $I = 594$ pA. The molecular assembly shows a flat-lying orientation on the HOPG surface. (c) Structural model for the type I arrangement.

by the achiral molecules were also observed. An STM image and the corresponding molecular model for the chiral domains are shown in Figure 5d,e.

The same molecular arrangements as those in the assemblies of P-18-PIMB and P-14-PIMB are observed in the adlayer of P-12-PIMB. Similar to the former two molecules, P-12-PIMB molecules self-organize into two types of arrangements with large-scale alternating bright and dark stripe domains in the packing geometries of (1) tail-to-tail and (2) tail-to-tail and intercalated alkyl chains (not shown here). The molecular bent directions in adjacent lamellae are antiparallel in both types of arrangements. The parameters in the two adlayers were measured.

To compare the adlayer structures, the parameters of various unit cells in the three self-assemblies are listed in Table 1. There are six unit cells in the three molecular assemblies. It can be seen that the adlayer structures vary with the change of chemical structures. The core parts of P-*n*-PIMB molecules are the same. The difference in the chemical structures among the three molecules is only the length of alkyl chains. Therefore, the *a* value in the unit cell parameters is constant at 0.8 ± 0.2 nm. On the other hand, with the decrease of *n* in P-*n*-PIMB molecules, the *b* value in the unit cell parameters is gradually reduced. However, the difference of the *b* value between the two types of arrangements is small, although the alkyl chains can take tail-to-tail and interdigitated arrangements. The structural flexibility of the molecules should be responsible for the interesting organization.

3. Gemini Surfactant. As a comparison, the assembling structure of a gemini surfactant OPD was investigated. Surfactant molecules could self-assemble into large-scale domains without structural defect, as shown in Figure 6a. The darker regions in the image correspond to the alkyl side chains of the molecules. The high-contrast stripes in the image correspond to π-conjugated moieties of the surfactant molecules, separated by the middle pentane spacer showing slightly dark variation in the contrast. This is depicted by an overlaid molecular model in Figure 6b. The molecules lie on the surface with the alkyl chains fully interdigitated. The molecular arrangement model in Figure 6c shows that the molecular aromatic parts constitute the bright band. The unit cell gives the parameters $a = 1.1 \pm 0.2$ nm, $b = 5.3 \pm 0.2$ nm, and $\alpha = 55 \pm 2°$, consistent with the STM measurement.

The aromatic moiety of the surfactant OPD is composed of two rigid aromatic groups connecting by a flexible pentane spacer and has a line-shape packing of dimeric aromatic moieties on the surface; for P-*n*-PIMB, the aromatic rings can form a bending conformation. This kind of banana-shaped molecular structure makes P-*n*-PIMB display more complicated assemblies. The molecular structures obviously dominate the assembling structures.

4. Driving Force. Understanding molecular ordering is a principal goal for surface physical chemistry. The competition between different interactions manifests itself in the existence of various phases of condensed matter systems. In this paper we have examined a 2D ordering in LC molecules arising from the competition among intermolecular interaction and molecule−substrate interaction. The molecules possess strong transverse dipoles in the bent core, and the strong cohesion resulting from the long-range dipolar forces induces the formation of molecular assembly.[3] On the other hand, the stability of the structure may be determined by the specific packing of banana-shaped molecules. Indeed, the banana-shaped molecules in the lamellae are approximately parallel, while they are antiparallel in neighboring lamellae. This kind of arrangement greatly decreases the molecular packing free space and results in a maximum of intermolecular interactions. In this way, a stable monolayer with a sufficiently low molecular lateral mobility is assembled. To understand the orientation between molecular assembly and the underlying HOPG surface, we acquired a composite STM image. Figure 7 presents a typical image in which the graphite lattice is shown simultaneously with the assembly of P-14-PIMB type II arrangement, and the azimuthal

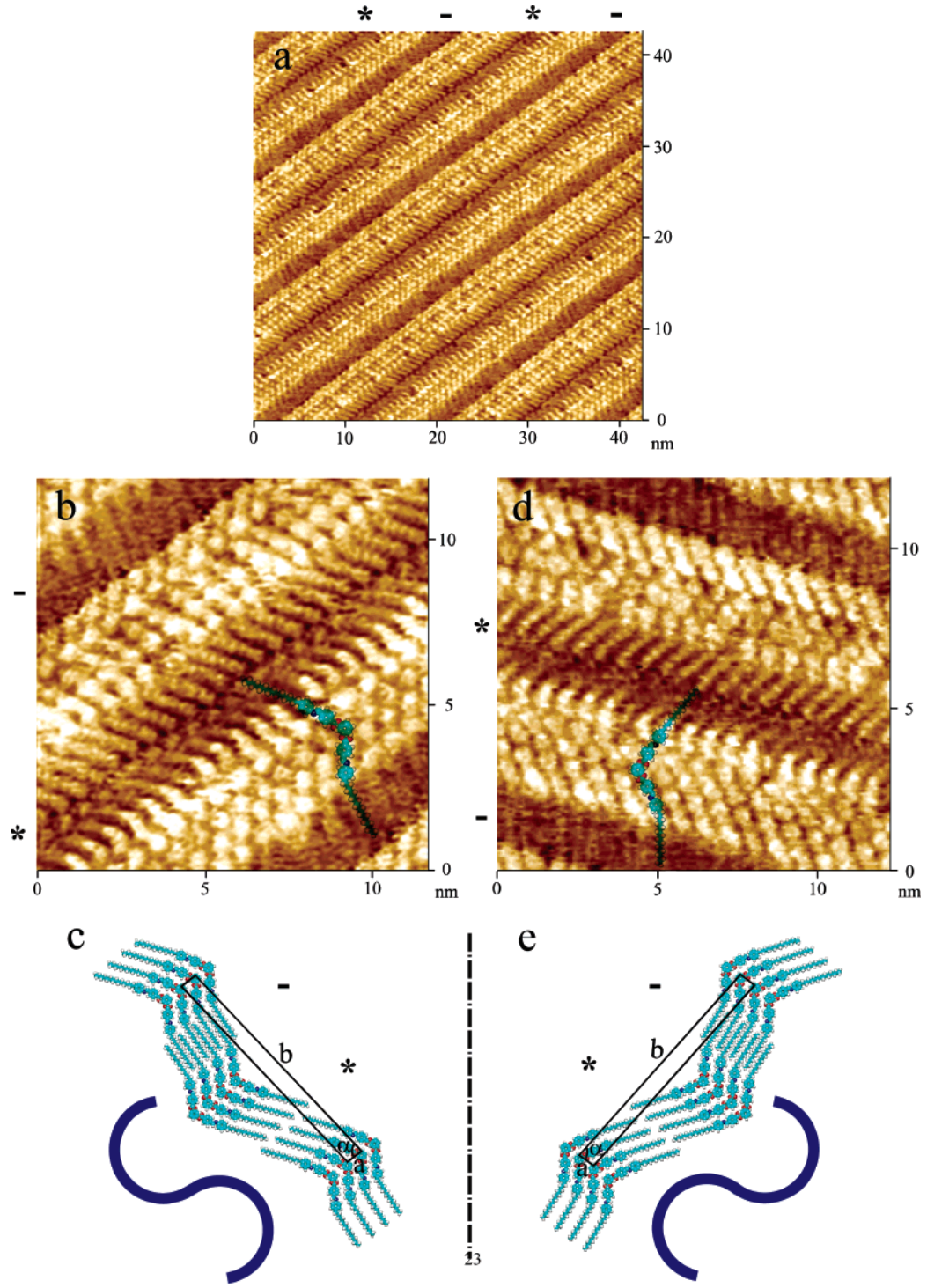

Figure 5. Type II adsorption geometry of P-14-PIMB molecules on the HOPG surface. (a) Large-scale STM image recorded with $V = 704$ mV, $I = 247$ pA. (b) and (d) High-resolution STM images showing mirror chiral structures by achiral molecules recorded with (b) $V = 704$ mV, $I = 247$ pA, and (d) $V = 715$ mV, $I = 759$ pA. (c) and (e) Structural models for the type II arrangements in (b) and (d), respectively, showing chiral domains.

TABLE 1: Unit Cell Parameters of P-*n*-PIMB

	C_{18}		C_{14}		C_{12}	
	I	II	I	II	I	II
a (nm)	0.8 ± 0.2	0.8 ± 0.2	0.8 ± 0.2	0.8 ± 0.2	0.8 ± 0.2	0.8 ± 0.2
b (nm)	11.5 ± 0.2	11.0 ± 0.2	10.6 ± 0.2	10.3 ± 0.2	10.3 ± 0.2	10.0 ± 0.2
α (deg)	85 ± 2	80 ± 2	87 ± 2	81 ± 2	86 ± 2	82 ± 2

angle of the assembly with respect to the substrate can be determined from this image. From the image, the azimuthal angle θ, which is the angle between direction b_1 and substrate lattice direction a_1, is estimated to be $166° \pm 2°$. The angles of α and β are measured to be $70° \pm 2°$ and $128° \pm 2°$, respectively, indicating an indefinite crystal relationship between the molecules and HOPG substrate. The indefinite relationship was also found in types I and II of the arrangements of P-*n*-PIMB ($n = 18$ and 12). The mismatch between the adlayer and substrate symmetry is an indication of relatively weak molecule−substrate interaction. The extents of intermolecular interdigitation and intermolecular reaction will affect the formation and stability of the self-assemblies. In the present study, it could be

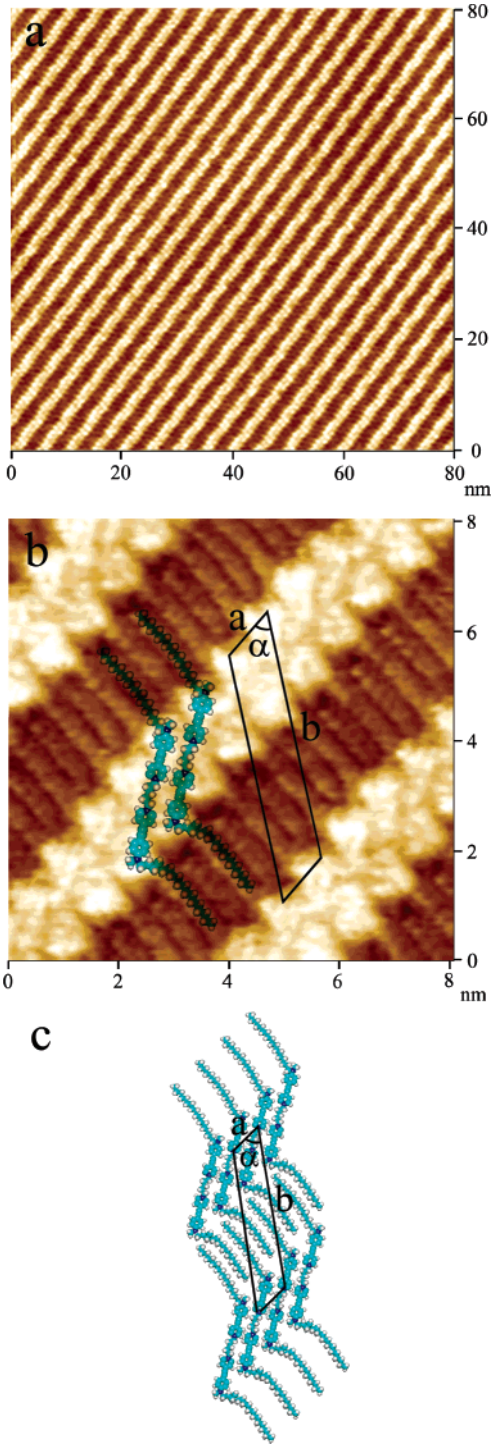

Figure 6. Gemini surfactant adlayer on the HOPG surface. (a) Large-scale STM image recorded with $V = 839$ mV, $I = 805$ pA. (b) High-resolution STM image recorded with $V = 839$ mV, $I = 867$ pA. (c) Structural model for the surfactant adlayer.

concluded that the packing structures are determined mainly by intermolecular interactions, while the molecule−substrate interaction seems to be of secondary importance.

Conclusion

The 2D assemblies of banana-shaped liquid crystal molecules, P-*n*-PIMB ($n = 18$, 14, and 12), on the HOPG surface are investigated by STM at the submolecular level. The results show two types of coexistent molecular arrangements of P-*n*-PIMB

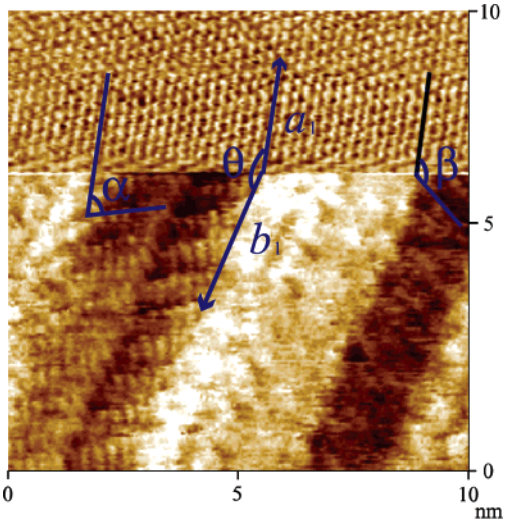

Figure 7. A composite STM image showing the orientation of the underlying HOPG lattice and the P-14-PIMB adlayer. In the present image, the scanning direction was from bottom to top. When scanning to half of the frame, we rapidly lowered the bias to a few millivolts from the normal hundreds of millivolts, and we increased the setpoint value to 1 nA. Therefore, the underlying HOPG lattice and the adsorbed molecular adlayer could be observed in the same image.

adlayers. The polarization of the P-*n*-PIMB monolayers is compensated by the adjacent lamellae with opposite bent direction in the two types of geometries. In the meantime, a bilayer structure of P-18-PIMB molecules is found. The orientation between the top and lower layers in the bilayer is directly determined by STM images. Owing to the flexible structure of the molecules, the banana-shaped LCs have a more complicated packing organization. The effect of molecular structure on the adlayer arrangement and the macroscopic property are demonstrated. On the HOPG surface, the packing structures of P-*n*-PIMB molecules are mainly determined by intermolecular reaction, while the molecule−substrate interaction seems to be of secondary importance. This surface microscopic assembling behavior of the P-*n*-PIMB molecules on HOPG might provide useful information in the application and theoretical research of liquid crystals.

Acknowledgment. Financial support from the National Natural Science Foundation of China (Nos. 20025308, 20177025, and 20121301), the National Key Project on Basic Research (Grants G2000077501 and 2002CCA03100), and Chinese Academy of Sciences are gratefully acknowledged. J.R.G. thanks S. B. Lei for experiments and Y. Yao for use of samples.

References and Notes

(1) O'neill, M.; Kelly, S. M. *Adv. Mater.* **2003**, *15* (14), 1135.
(2) Grell, M.; Bradley, D. D. C. *Adv. Mater.* **1999**, *11* (11), 895.
(3) Niori, T.; Sekine, T.; Watanabe, J.; Furukawa, T.; Takezoe, H. *J. Mater. Chem.* **1996**, *6*, 1231.
(4) Watanabe, J.; Niori, T.; Sekine, T.; Takezoe, H. *Jpn. J. Appl. Phys.* **1998**, *37*, L139.
(5) Kentischer, F.; MacDonald, R.; Warnick, P.; Heppke, G. *Liq. Cryst.* **1998**, *25*, 341.
(6) Sekine, T.; Niori, T.; Sone, M.; Watanabe, J.; Choi, S. W.; Takanishi, Y.; Takezoe, H. *Jpn. J. Appl. Phys.* **1997**, *36*, 6455.
(7) Moncton, D. E.; Pindak, R.; Davey, S. C.; Brown, G. S. *Phys. Rev. Lett.* **1982**, *49*, 1865.
(8) Scott, J. F. *Phase Transitions* **1991**, *30*, 107.
(9) Scott, J. F.; Duiker, H. M.; Beale, P. D.; Pouligny, B.; Dimmler, K.; Parris, M.; Butter, D.; Eaton, S. *Physica B* **1988**, *150*, 160.
(10) Bune, A. V.; Fridkin, V. M.; Ducharme, S.; Blinov, L. M.; Palto, S. P.; Sorokin, A. V.; Yudin, S. G.; Zlatkin, A. *Nature* **1998**, *391*, 874.

(11) Lemieux, R. P. *Acc. Chem. Res.* **2001**, *34* (11), 845.
(12) Whitesides, G. M.; Boncheva, M. *Proc. Natl. Acad. Sci. U.S.A.* **2002**, *99*, 4769.
(13) Yoshimoto, S.; Higa, N.; Itaya, K. *J. Am. Chem. Soc.* **2004**, *126* (27), 8540.
(14) Miura, A.; Chen, Z.; Uji-i, H.; De Feyter, S.; Zdanowska, M.; Jonkheijm, P.; Schenning, A. P. H. J.; Meijer, E. W.; Wurthner, F.; De Schryver, F. C. *J. Am. Chem. Soc.* **2003**, *125* (49), 14968.
(15) Hipps, K. W.; Scudiero, L.; Barlow, D. E.; Cooke, M. P., Jr. *J. Am. Chem. Soc.* **2002**, *124* (10), 2126.
(16) Xu, Q. M.; Wang, D.; Wan, L. J.; Wang, C.; Bai, C. L.; Feng, G. Q.; Wang, M. X. *Angew. Chem. Int. Ed.* **2002**, *41* (18), 3408.
(17) Gong, J. R.; Wan, L. J.; Yuan, Q. H.; Bai, C. L.; Jude, H.; Stang, P. J. *Proc. Natl. Acad. Sci. U.S.A.* **2005**, *102* (4), 971.
(18) Spong, J. K.; Mizes, H. A.; Lacomb, L. J., Jr.; Dovek, M. M.; Frommer, J. E.; Foster, J. S. *Nature* **1989**, *338*, 137.
(19) Smith, D. P. E.; Hörber, H.; Gerber, C.; Binnig, G. *Science* **1989**, *245*, 43.
(20) Foster, J. S.; Frommer, J. E. *Nature* **1988**, *333*, 542.
(21) Smith, D. P. E.; Hörber, J. K. H.; Binnig, G.; Nejoh, H. *Nature* **1990**, *344*, 641.
(22) Askadskaya, L.; Boeffel, C.; Rabe, J. P. *Phys. Chem.* **1993**, *97* (3), 517.
(23) Charra, F.; Cousty, J. *Phys. Rev. Lett.* **1998**, *80* (8), 1682.
(24) Wu, P.; Zeng, Q. D.; Xu, S. D.; Wang, C.; Yin, S. X.; Bai, C. L. *ChemPhysChem* **2001**, *12*, 750.
(25) Hara, M.; Iwakabe, Y.; Tochigi, K.; Sasabe, H.; Garito, A. F.; Yamada, A. *Nature* **1990**, *344*, 228.
(26) Hara, M.; Umemoto1, T.; Takezoe1, H.; Garito, A. F.; Sasabe, H. *Jpn. J. Appl. Phys.* **1991**, *30*, L2052.
(27) Niori, T.; Adachi, S.; Watanabe, J. *Liq. Cryst.* **1995**, *19* (1), 139.
(28) Quagliotto, P.; Viscardi, G.; Barolo, C.; Barni, E.; Bellinvia, S.; Fisicaro, E.; Compari, C. *J. Org. Chem.* **2003**, *68*, 7651.
(29) Tang, Y.; Wang, Y.; Wang, G.; Wang, H.; Wang, L.; Yan, D. *J. Phys. Chem. B* **2004**, *108* (34), 12921.
(30) Khachaturyan, A. G. *J. Phys. Chem. Solids* **1975**, *36*, 1055.